

## Research Paper

# A fully automated measurement system for the characterization of micro thermoelectric devices near room temperature

Amit Tanwar<sup>a</sup>, Swatchith Lal<sup>a</sup>, Rajvinder Kaur<sup>a</sup>, N. Padmanathan<sup>a</sup>, Eric Dalton<sup>b</sup>, Kafil M. Razeeb<sup>a,\*</sup>

<sup>a</sup> Micro-Nano Systems Centre, Tyndall National Institute, University College Cork, Dyke Parade, Lee Maltings, Cork T12 R5CP, Ireland

<sup>b</sup> Bernal Institute, Stokes Laboratories, University of Limerick, Limerick, Ireland

## ARTICLE INFO

## Keywords:

Thermoelectric devices (TEDs)  
Thermal resistance  
Cooling power  
COP  
Measurement system

## ABSTRACT

In this work, we report the customized design and development of a fully automated measurement system to characterize the temperature-dependent properties of microscale thermoelectric devices. The featured system can characterize the devices up to a dimension of  $8.79 \times 8.79 \text{ mm}^2$  in an atmospheric environment. Commercially available bismuth telluride-based thermoelectric modules (both thermoelectric generator and thermoelectric cooler) are used to validate the feasibility and accuracy of the developed system. Their performance data is analysed and compared with the available manufacturer datasheet. The measured data from these devices are found to be in good agreement with the anticipated values and showed an acceptable deviation of less than 4% in the output performances. The developed setup is simple to operate and suitable for performance evaluation of both macro and micro-thermoelectric devices. The system accurately reproduces application conditions the module may be subjected to in a real-world environment.

## 1. Introduction

Thermoelectric devices (TEDs) are one of the most attractive technologies which are capable of converting waste heat into electricity and vice versa. A thermoelectric device consists of several p and n-type semiconducting thermocouples connected electrically in series and thermally parallel. TEDs work without any moving parts, noiseless, low complexity, no requirement for specific maintenance, and is eco-friendly [1]. These TEDs can be divided into two different types based on the application as shown in Fig. 1. First, as a thermoelectric generator (TEG), which is based on the Seebeck effect and can convert thermal energy into electric energy. Second, as a thermoelectric cooler (TEC), which is based on the Peltier effect and can convert electric energy into thermal energy (heating or cooling).

In recent years, microscale TEGs are being used as a potential energy source for the internet of things (IoT) [2], wireless sensor [3], and wearable health care devices [4,5], which are mainly works at a low temperature gradient ( $\leq 50 \text{ K}$ ). Because of their low-temperature gradient sensitivity and low power output, the precise measurement of these micro-thermoelectric generators ( $\mu$ -TEGs) is challenging, and the conventional thermoelectric device characterization system comprises a

Peltier module and a heat sink for heating and cooling [6,7] which is not capable enough to determine the thermal resistance, thermal conductivity and efficiency of the TEG devices. Therefore, an explicit device characterization system becomes crucial to measure the thermoelectric parameters i.e., output voltage, electrical resistance, current and output power of the  $\mu$ -TEGs, especially at low-temperature gradients [5,8].

To evaluate the dimensional figure-of-merit ( $zT$ ) of the TEGs and coefficient of performance (COP) of TECs, the measurement setup needs special requirements such as a heat flow meter, a load cell to monitor the applied pressure on devices, precise temperature controller on both side of the device to create desired temperature gradient. Recently, Dasgupta and Umaraji [9] designed an instrument based on the parallel heat-flow technique to measure the thermal conductivity and the Seebeck coefficient for a minimum sample size of  $1 \times 1 \times 10 \text{ mm}^3$  for a temperature range from room temperature to 700 K. The authors measured the thermal conductivity of fused silica, which is within  $\pm 5\%$  of the absolute value. Meantime, Kraemer and Chen [10] demonstrated a method to characterize bulk TEG devices and the experiment is based on the differential technique that are direct and absolute within the measurement error below 3%. However, there is no provision to measure the sample thickness in situ and to reduce the thermal resistance by applying

\* Corresponding author.

E-mail address: [kafil.mahmood@tyndall.ie](mailto:kafil.mahmood@tyndall.ie) (K.M. Razeeb).

the pressure. Furthermore, Liu et al. [11] reported an instrument that can characterize the TEG up to a size of  $60 \times 60 \text{ mm}^2$ . The hot side of the proposed system can reach a temperature up to  $500 \text{ }^\circ\text{C}$ , while the cold side can be set to temperature between ambient and  $100 \text{ }^\circ\text{C}$ . Meanwhile, Hejtmánek et al. [12] developed a system for validating TEG devices under a wide range of temperatures ( $T_{\text{cold}} = 25 \text{ }^\circ\text{C}$  to  $90 \text{ }^\circ\text{C}$ ,  $T_{\text{hot}} = 450 \text{ }^\circ\text{C}$ ) and mechanical loading ( $P = 0 \text{ N}$  to  $10^4 \text{ N}$ ). Beretta et al. [13] also reported a TEG measurement system with a temperature interval of  $25\text{--}150 \text{ }^\circ\text{C}$ , and they tested the system with a commercial TEG and demonstrated  $< 5\%$  error in the power output. The compressive force across the module should be continuously monitored and adjusted because it can vary during the measurement. Because, the non-uniform force can damage the module, or leads to an error in the measurement. However, the above systems [11–13] are using the manual compression screw to apply force on the TEG where it is hard to auto-adjust the force during the measurement.

Moreover, thermoelectric coolers (TEC), also known as heat pumps, are getting more interest in thermal management of electronic and photonic chips [14–17]. Depending upon the applied current's direction, a TEC can be used either for cooling or heating. For TEC's optimum performance, it is necessary to remove the heat from the hot side. To date, various customized measurement systems are proposed based on direct-contact and non-contact approaches for the TEC's performance evaluation. In direct-contact measurement, a TEC device is sandwiched between the Q-meter (heat flow meter) as the hot side and a copper block as the cold side (heat sink). The  $\Delta T$  across the Q-meter is measured using four thermocouples placed on the Q-meter separated by accurately determined distances [14]. A similar kind of setup is used by Bulman et al. [18], in which they placed the TE device on top of a Q-meter. Heat is applied to the top side of the TEC device using a resistive heater. On the other hand, the non-contact measurement technique uses infrared radiation [18] or laser irradiation [17] instead of a heater to supply the heat flux and uses an infrared camera [19] or thermoreflectance microscopy [20] to measure the temperature at the top of the TEC device. To the best of our knowledge, there is no specified single instrument to characterize both  $\mu$ -TEG and  $\mu$ -TEC. In this direction only minimal effort have been devoted to make a unique characterization setup for micro-scale thermoelectric devices.

Thereby, this work aims to design and develop a fully automated characterization apparatus based on the ASTM-D5470-06 [21] method for micro-thermoelectric devices (both generators and coolers), which allows a reliable and fast measurement of the  $\mu$ -TEDs performance. The proposed setup is an integrated data acquisition system equipped with

dedicated hardware and software developed in LabVIEW, which enables the user to fully control the setup parameters for the measurements and ensure the real-time output data acquisition using data acquisition systems (DAQ). Finally, the system validation and characterization of commercial micro-thermoelectric modules are demonstrated.

## 2. System design

An overview of the  $\mu$ -TEG characterization setup is shown in Fig. 2 (a). The whole system is constructed on a  $300 \times 300 \times 12.7 \text{ mm}^3$  aluminium breadboard. Two copper meter bars  $100 \text{ mm}$  long and  $12.7 \text{ mm}$  diameter having a thermal conductivity of  $401 \text{ W m}^{-1} \text{ K}^{-1}$  (Good-fellow) are used. The lower meter bar is mounted on the top surface of a Peltier device of  $50 \times 50 \times 5.3 \text{ mm}^3$  (ThorLabs, TECL4) and used to provide the cold junction to the specimen surface. Eight negative temperature coefficient (NTC) thermistors of value  $10 \text{ k}\Omega$  with an accuracy of  $\pm 0.01\%$  and  $2.6 \text{ mm}$  diameter are placed in the meter bars to measure the temperature across the bars. The temperature range of these thermistors are from  $0$  to  $150 \text{ }^\circ\text{C}$ . The resistances of all thermistors are recorded using two NI-9219 DAQ-cards. One resistive cartridge heater of  $15 \text{ W}$  (HT15W from ThorLabs) with a diameter of  $3.1 \text{ mm}$  and  $12.7 \text{ mm}$  long is placed inside the top side of the upper bar. The upper bar is attached to a Kistler's Strain gauge load cell (4576A2NC3) with a rated load of  $2 \text{ kN}$ . The block consisting of load cell and the upper bar is attached with a MSL lead screw linear actuator of  $100 \text{ mm}$  travel range with a resolution of  $\pm 0.22 \mu\text{m}$ . A micro-optical laser micrometre is used to measure the thickness of the sample from  $0$  to  $28 \text{ mm}$  with a resolution of  $\pm 0.44 \mu\text{m}$ . A steel rod of diameter  $12.7 \text{ mm}$  and length  $100 \text{ mm}$  is mounted normal to the micrometre beam to measure the thickness of the sample.

The contact surfaces of both the copper bars are polished to get a mirror finish. It is desirable to have a low roughness for the contacting surfaces of the meter bars to reduce thermal contact resistances and have proper contact. The surface roughness is measured with the atomic force microscope (AFM). Fig. 2 (b & c) shows the representative AFM topographic images of the surface roughness profile of the copper bar. The root-mean-square (RMS) roughness is found to be  $26.2 \text{ nm}$ , which is comparable to the roughness of the another system previously developed by the group [22].

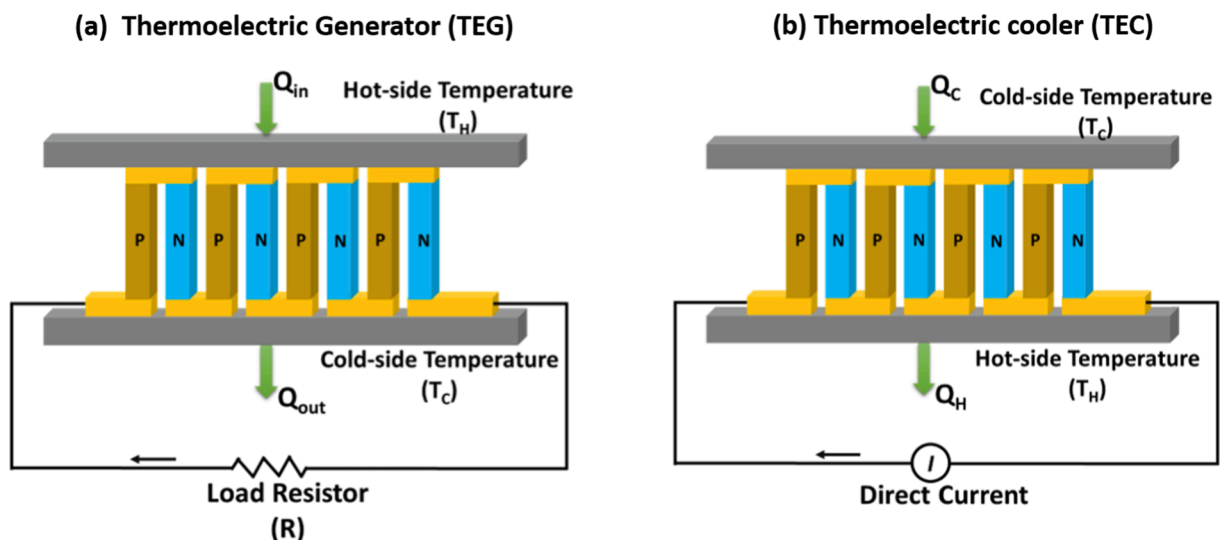


Fig. 1. Schematic showing the (a) Thermoelectric generator (TEG) based on Seebeck effect, (b) Thermoelectric cooler (TEC) based on Peltier effect.

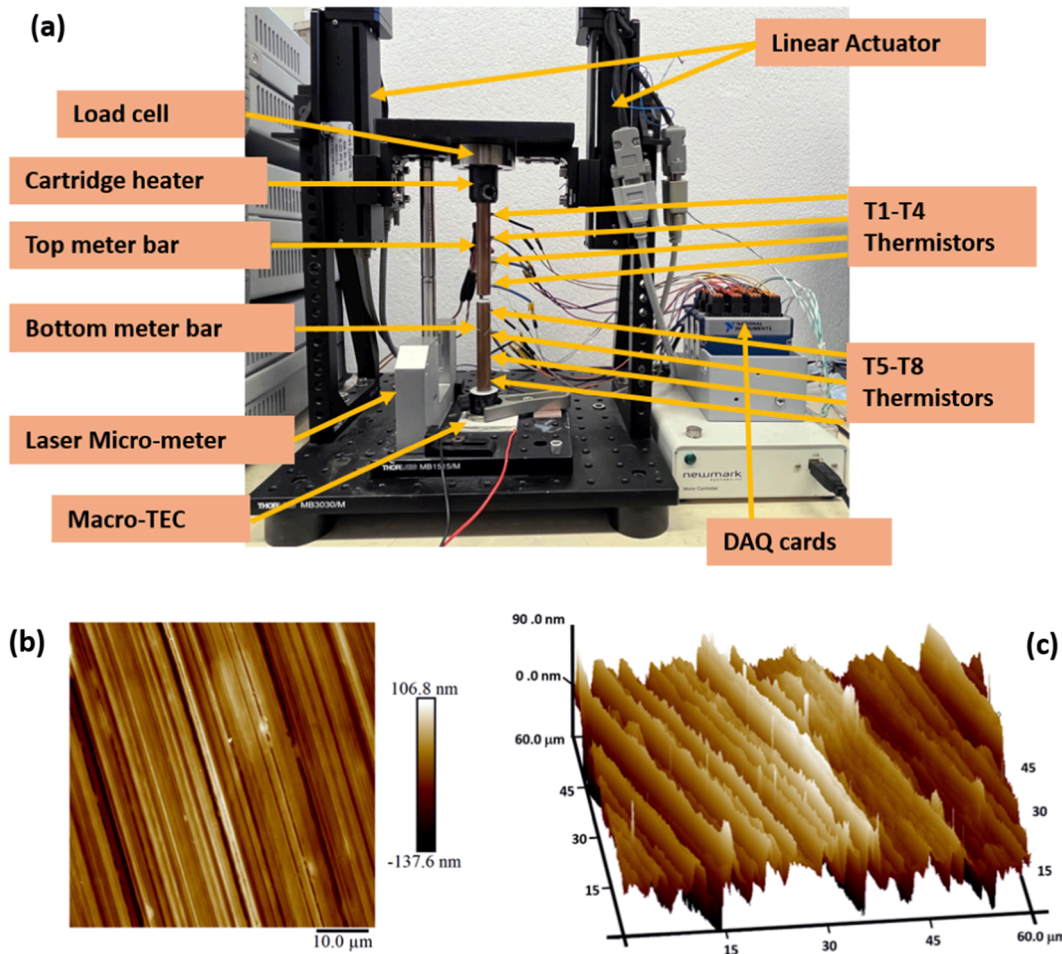


Fig. 2. (a) Thermoelectric measurement system (b) Topographic and (c) 3D topographic surface roughness profile of the copper bar surface.

### 3. Theory and measurement method

#### 3.1. ASTM D5470-06 technique principle

The thermal conductivity of the specimen is measured based on the ASTM D5470-06 method [21]. ASTM D5470-06 technique is an extended version of the ASTM D5470 method with the added external force and in-situ thickness measurement of the sample. This standard is based on the idealized one-directional heat flow between two parallel meter bars, separated by a test specimen of uniform thickness. The thermal gradient imposed between the two-meter bars causes heat flow through the specimen. The heat flow is perpendicular to the specimen surfaces and is uniform across the surfaces with no lateral heat spreading. The schematic representation of ASTM D5470 method with two-meter bars and heat flow equation is shown in Fig. 3. In this setup, heat is supplied from the top side of the upper bar and dissipated at the lower meter bar. Eight thermistors are placed inside the two-meter bars (4 in each) at a uniform distance to measure the local temperature. Once the steady-state heat flow is reached, the temperatures of both upper- and lower-meter bars are recorded. These temperatures are used to extrapolate the temperature at the contact surfaces of each bar. Moreover, with accurate values of meters' bars, the heat conduction through the specimen can be calculated. The apparent thermal resistance (RA), often called thermal impedance can be calculated from the temperature drop caused by the sample using its geometry and given as [23]:

$$RA = \frac{A(T_H - T_C)}{\dot{Q}} \quad (1)$$

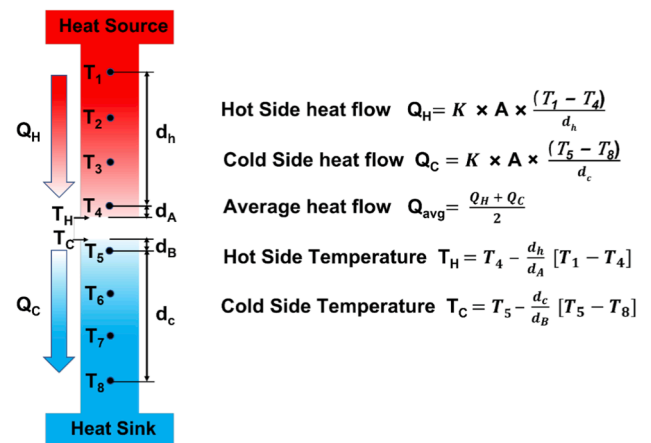


Fig. 3. The measurement setup for the ASTM D5470-06 standard test setup.

where  $A$  is the cross-sectional area of the meter bars,  $T_H$  and  $T_C$  are the extrapolated hot and cold surface temperatures respectively and  $\dot{Q}$  is the heat flow rate.

The apparent thermal conductivity of the specimen can be obtained by plotting thermal impedance against the thickness of the specimen and is given by:

$$k = \frac{Ql}{A(T_H - T_C)} = \frac{t}{RA} \quad (2)$$

where  $t$  is the thickness of the specimen.

### 3.2. Principles of TED module measurement

The TED measurement system includes a personal computer to control the setup through General Purpose Interface Bus (GPIB) and an Agilent power supply connected to Cartridge heater to provide the heat to the top meter bar. This developed system allows the characterization of the TED module up to a size of  $8.79 \times 8.79 \text{ mm}^2$  from room temperature up to a temperature difference of 75 K. During the measurement, the TED module is placed in between two meter bars. The complete schematic description of the developed micro-TED measurement setup with a control feedback circuit by a computer is shown in Fig. 4. The upper meter bar is connected to a stepper-motor-controlled linear actuator, which allows change in position with a precision of  $0.22 \mu\text{m}$  and allows applying and controlling the pressure on the hot side of the device. A compressive load attached to the top bar is used to reduce the interface gaps and thermal contact resistances. However, excess pressure on the micro-thermoelectric devices can break the device and it is essential to optimize the compressive pressure for the characterization of the device. The applied pressure on the sample is measured with a Kistler's strain gauge load cell with a rated load of 2 kN with an accuracy of  $\pm 0.25\%$ . Strain gauges are applied to the flexural diaphragms in the load cell and deliver a bridge output voltage that is directly proportional to the measurand during concentric load application. The sensitivity of the load cell is  $1.5 \text{ mV/V}$ . The contact pressure on the sample can be automatically adjusted with the feedback loop.

An optical laser micrometre (MicroU) is used to measure the thickness of the sample in-situ as this method has advantages over linear variable differential transformer (LVDT) or other traditional micrometres due to its non-contact nature, which has no abrasion on the surface of the measured object. Before sample insertion, the micrometre is initialized to zero by bringing the two meters into contact. The sample thickness up to 28 mm with a resolution of  $0.44 \mu\text{m}$  can be measured by this micrometre.

The output voltage and electrical resistance of the TEG module are acquired in real-time using a digital multimeter (Agilent 34401A). In order to determine the energy balance accurately, both heat flux entering the thermoelectric module  $Q_{in}$  and heat flux released by the module  $Q_{out}$  are measured. The TEG module's performance can be

measured by keeping the cold surface temperature,  $T_C$ , constant at a reference value while varying the hot side temperature to achieve the desired  $\Delta T$ .

The developed system can be used to determine the following parameters of a TEG:

- Open circuit voltage
- Short circuit current
- Internal electrical resistance as a function of Temperature
- Thermal resistivity/Conductivity of the device
- Effective overall device Seebeck coefficient
- Power output
- Energy conversion efficiency

The temperature of the hot side,  $T_H$ , and the cold side,  $T_C$ , can be automatically controlled by closed-loop program in LabVIEW software. Once a constant  $\Delta T$  is maintained, voltage developed across the TEG is measured. The effective Seebeck coefficient ( $\alpha$ ) can be calculated using the following equation:

$$\alpha = \frac{\Delta V}{\Delta T} \tag{3}$$

where  $\Delta V$  is the voltage developed in the TEG and  $\Delta T$  is the temperature gradient across the TEG. The output electrical power generated by TEG module is determined from both output voltage and the measured current. The internal resistance of the module is calculated using the following equation:

$$R_{in} = \frac{V_{oc}}{I_{sc}} \tag{4}$$

where  $V_{oc}$  is the open circuit voltage and  $I_{sc}$  is the short-circuit current. The conversion efficiency of the TEG module can be defined as the ratio of the generated power output ( $P_{out}$ ) to the incoming heat ( $Q_{in}$ ).

$$\eta = \frac{P_{out}}{Q_{in}} \tag{5}$$

The thermal resistance is defined as the ratio of the temperature difference between the top and bottom surfaces of the device to the rate of heat flow ( $\dot{Q}$ ). The thermal resistance ( $R_{th}$ ) is given as:

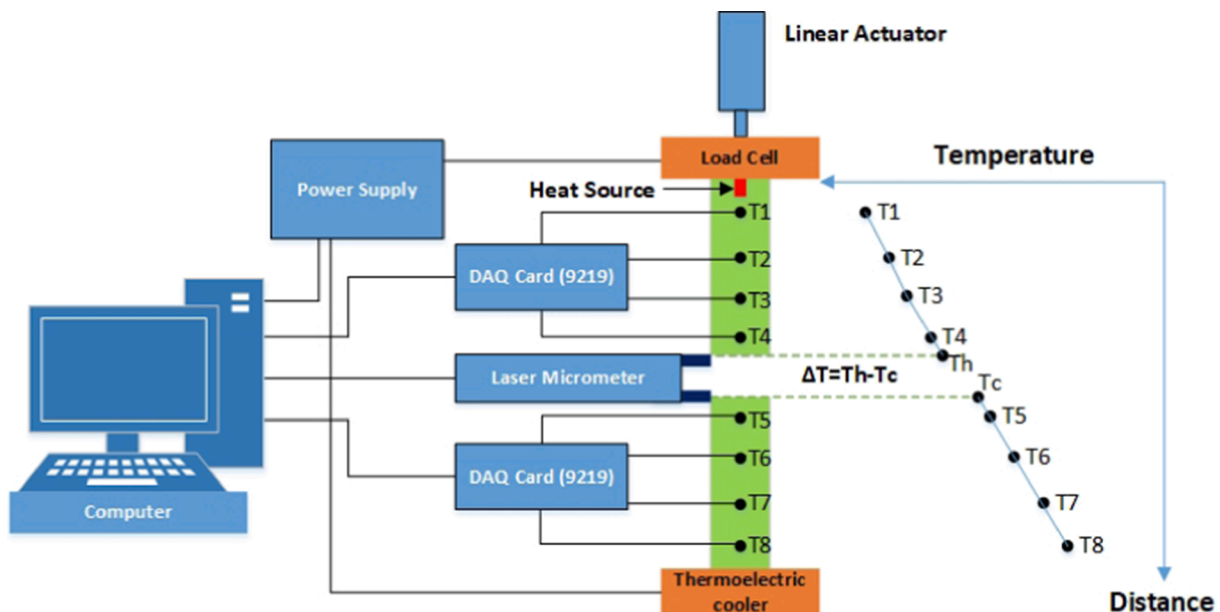


Fig. 4. Schematic of instrumentation and control of the experimental facility.

$$R_{th} = \frac{(T_H - T_C)}{\dot{Q}} \quad (6)$$

While, the thermal conductivity of the device can be calculated using Fourier's law of heat conduction:

$$k = \frac{\dot{Q}L}{A\Delta T} \quad (7)$$

where  $\dot{Q}$  is rate of heat flowing through the device,  $A$  and  $L$  is the cross-sectional area and thickness of the device respectively, and  $\Delta T$  is the temperature difference across the device. Traditionally, the performance of the thermoelectric cooler (TEC) is defined by two major parameters: cooling power ( $Q_c$ ) and coefficient of performance ( $COP$ ). Where  $Q_c$  can be defined as the heat removed by the TEC from a heat source, and  $COP$  is the amount of cooling power divided by input electrical energy and  $COP$  can be defined by the following equation:

$$COP = \frac{Q_c}{W} \quad (8)$$

where  $W$  is the input power in Watt.

An algorithm is developed for measuring and recording the experimental parameters, as shown in Fig. 5. According to the algorithm, once the sample is sandwiched between two metre bars and with desired user inputs such as applied load and  $\Delta T$ , the hot and cold side surface temperature difference of the meter bars are continuously measured. When the thermal stability is attained with the desired tolerance of  $\pm 0.1$  °C from the required  $\Delta T$ , the output performance of the TEG device such as output power, voltage, electrical resistance, thermal resistance and thermal conductivity are measured. The measurement process can be repeated for the other applied load and  $\Delta T$ . By using the measurement for desired load and  $\Delta T$ , the output parameter for TED module is recorded, and the system automatically shuts down. The measurement and the control of the entire system are automated using LabVIEW developed program as shown in Fig. 6.

## 4. Results and discussion

### 4.1. Contact measurement

For near room temperature measurements, the sensitivity and precision of the measurement system are critical to provide reliable and accurate properties of the micro-thermoelectric device. In order to validate the sensitivity and precision of the developed system, the temperature difference between the two surfaces of the copper meter bars at self-contact mode is measured. Usually, temperature drop across the two contact is primarily associated to the roughness of the surfaces because it is not possible to have an atomically smooth contact between

the two surfaces. It is always desirable to use some thermal paste and apply nominal pressure to eliminate the air voids between the two contact surfaces. In this work, measurements are performed in dry contact as well in wet contact mode as a thermal paste (Arctic Silver 5) is applied between the two-meter bars to reduce the contact resistance. Temperature distribution in the meter bars for both cases are recorded by eight thermistors embedded and shown in Fig. 7(a), when a low heat flux (0.2010 W) and a constant pressure of 50 kPa is applied to the bars. Both the graphs show a linear temperature distribution for both the bars. The surface temperatures ( $T_H$  and  $T_C$ ) are extrapolated from these recorded values. Wet contact measurement shows a low temperature difference of 0.089 °C as compared to dry contact of 0.217 °C. So, by using thermal paste, the thermal contact resistance can be reduced and the system can achieve the temperature difference with a maximum deviation of 0.089 °C.

### 4.2. Thermal conductivity measurement

Validation of the developed system is carried out by measuring the thermal conductivity of three circular aluminum (Al) disks of diameter 12.7 mm with different thicknesses of 1.15 mm, 3 mm, and 6 mm (Goodfellow, Product Code: AL00-RD-000113). The thermal conductivity of Al is  $237 \text{ Wm}^{-1}\text{K}^{-1}$  in a temperature range of 0–100 °C from the manufacturer's datasheet. A thin layer of arctic silver paste is applied as a thermal paste onto both surfaces of the disk to minimize the thermal contact resistance. The measurements are conducted at room temperature and under 50 kPa constant pressure. The recorded measurement of each disk for thermal impedance against their thickness is plotted in Fig. 7(b). The thermal conductivity of the Al disk is calculated by inverting the slope of the fitted line. The estimated thermal conductivity is calculated to be  $238.26 \text{ Wm}^{-1}\text{K}^{-1}$ , which is about 0.53% higher than the manufacturer datasheet value.

### 4.3. Commercial TEG module measurement

In order to determine the capability of the system to measure the performance of micro-TEGs, a commercial TEG of  $8.79 \times 8.79 \text{ mm}^2$  model No. NL1022T-05AC of Marlow Industries, Inc. is used to measure its output performance with respect to temperature. The TEG device is sandwiched between the two copper meter bars and to reduce the thermal contact resistance and to ensure proper contact, a thin layer of thermal conductive paste (Arctic Silver 5) is coated on both sides of the device and a constant pressure of 50 kPa is applied. During the measurement, the cold side temperature is fixed at 27 °C, whereas the hot side temperature is varied from 27 °C to 65 °C. The temperature fluctuation is set to less than 0.1 °C while recording the output values. Measurement repeatability is ensured by loading and unloading the

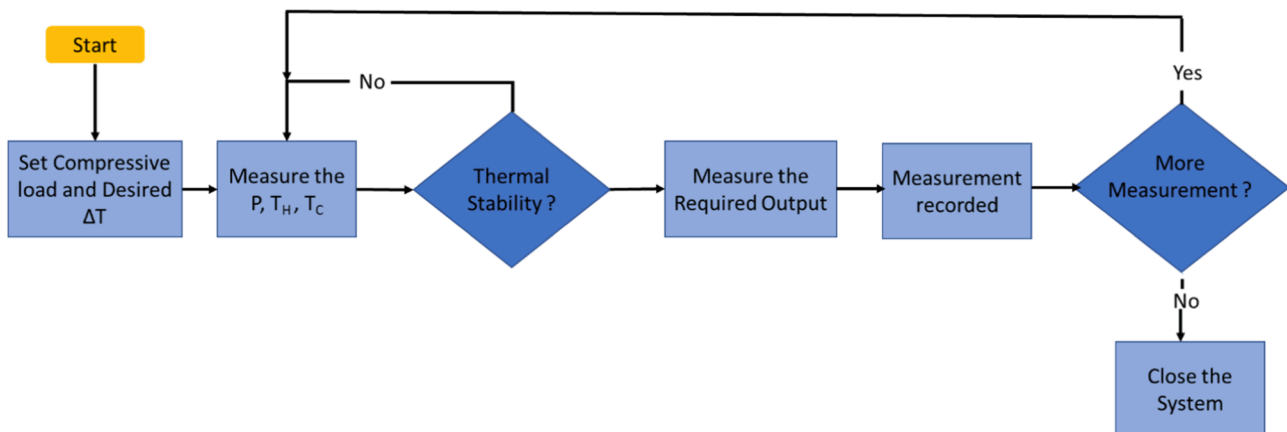


Fig. 5. Flow Chart for the measurement of output parameters of the TED tested using the developed setup.

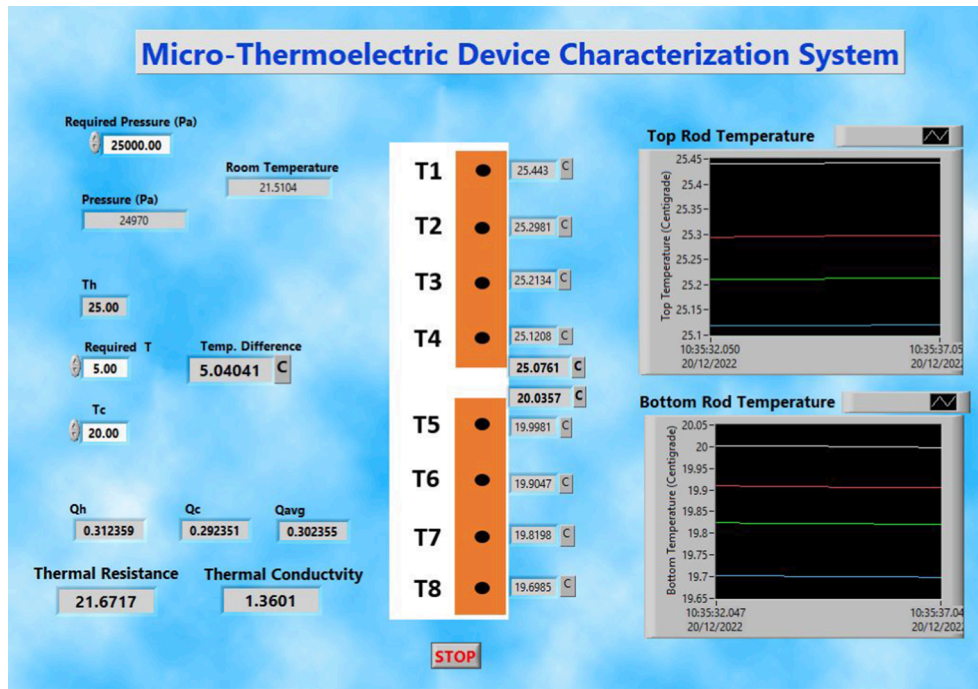


Fig. 6. LabVIEW interface programme to control and record the measurement.

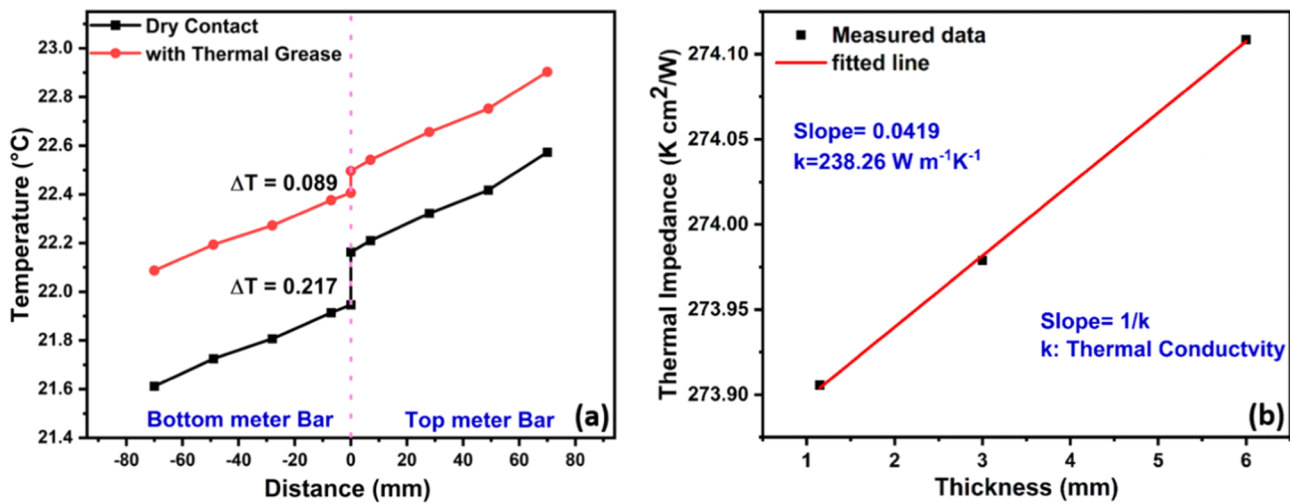


Fig. 7. (a) Temperature distribution across each metre-bar, (b) Thermal impedance as a function of thickness of Al disk.

device at fixed applied pressure for 3 times (M1, M2, and M3) and it demonstrated good repeatability. The measured output voltage as a function of temperature for three different cycles is shown in Fig. 8(a). The mean values of all three measurements (M1, M2 and M3) are compared with the provided values as shown in Table 1.

The datasheet of the commercial TEG provided output voltages only for two hot side temperatures i.e., 35 and 55 °C. It is apparent that the data provided by the manufacturer and the output voltage measured from this work differ slightly. This is because manufacture data refer to a different measurement condition in which nitrogen gas ambient is used for their measurements. Only < 3.5% of deviation from the reported values is observed. In order to determine the voltage versus current curve (*I-V*) of the thermoelectric generator, an external resistor is used as a load to measure the output voltage, as a function of output current for different temperature gradients ( $\Delta T$ ) ranging from 5 to 20 K. Typical *I-V* curves are shown in Fig. 8(b), which demonstrates a linear behaviour for

all the temperatures, and shows that the internal resistance of the TEG has a linear relation with the temperature gradient. The effective Seebeck coefficient of the TEG is calculated as  $12.52 \pm 0.13$  mV/K from Fig. 8(a) using equation (3). Unfortunately, there is no available Seebeck value in the manufacturer datasheet for comparison. Fig. 8(c) shows the output power (*P*) as a function of current at different temperature gradients. From the *P-I* characteristic graph, a maximum power output of 0.355, 1.26, 2.94 and 5.07 mW is observed for the temperature gradients of 5, 10, 15 and 20 K, respectively.

Also, the thermal resistance and thermal conductivity of the TEG are measured for two selected temperature gradients ( $\Delta T$ ). When cold side and hot side temperatures are fixed at 27 °C and 35 °C, the measured thermal conductivity profile is shown in Fig. 8(d). The measured thermal resistance and thermal conductivity are  $19.95\text{--}20.16$  KW<sup>-1</sup> and  $1.37\text{--}1.40$  Wm<sup>-1</sup>K<sup>-1</sup> respectively, which are in good agreement with the datasheet values. At  $\Delta T = 8$  K, the reported thermal resistance and

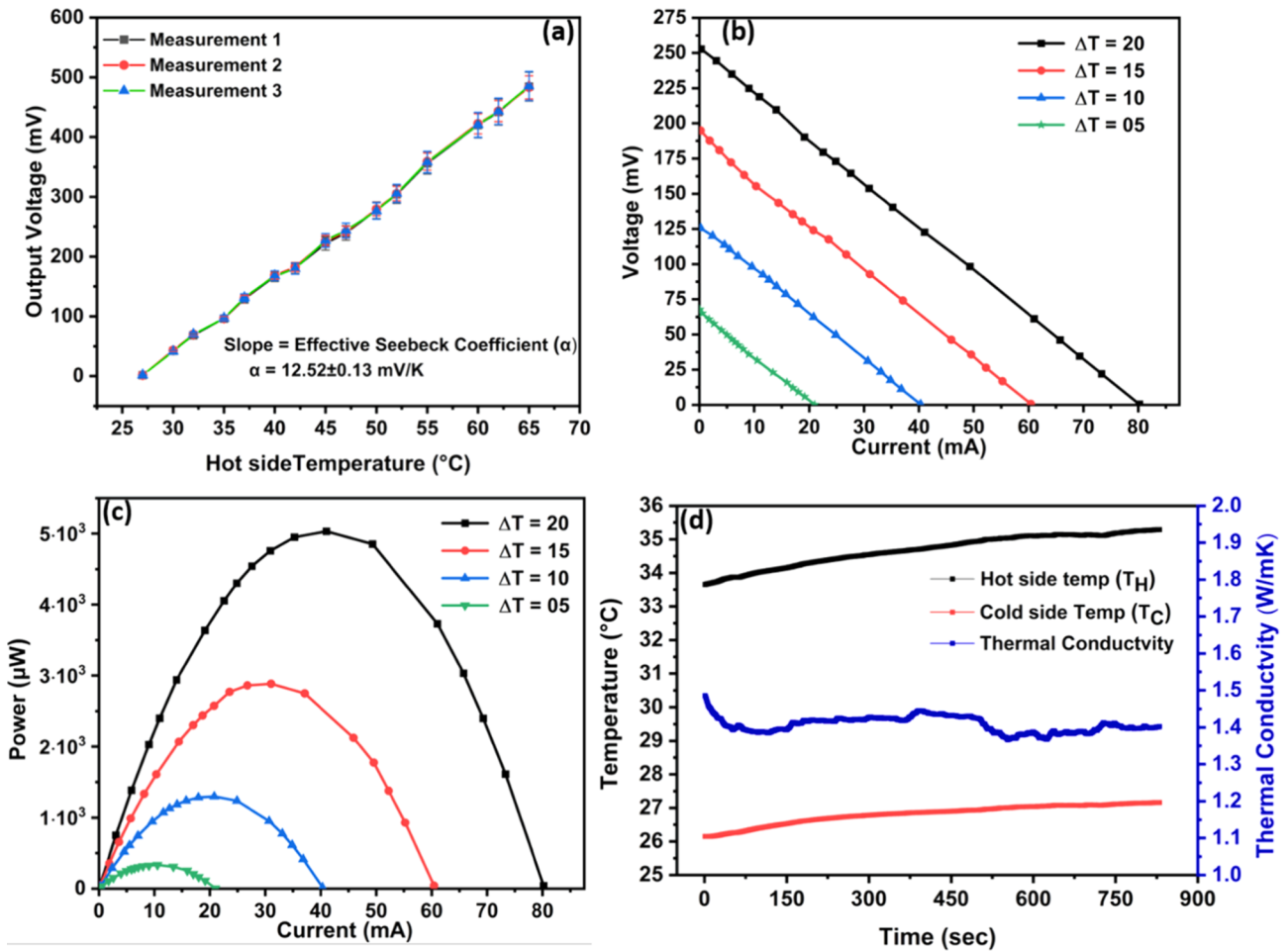


Fig. 8. (a) Output voltage vs. hot side temperature, (b)  $I$ - $V$  curve for four-different temperature gradients, (c)  $P$ - $I$  curve for four-different temperature gradient, (d) Fixed cold side, hot side temperatures, and thermal conductivity as a function of time.

Table 1  
Output voltage measurement from this work and manufacturer datasheet.

Hot side Temperature (°C)	M1 (mV)	M2 (mV)	M3 (mV)	Mean of measurement (mV)	Datasheet (mV)	Deviation (%)
35	96.30	96.50	96.90	96.57	100	3.43
55	356.25	359.00	358.20	357.82	370	3.29

thermal conductivity of the device are  $20.77 \text{ KW}^{-1}$  and  $1.37 \text{ Wm}^{-1}\text{K}^{-1}$  respectively. However, some discrepancies are observed in experimental values due to commonly overlooked inaccuracies (e.g., a layer of thermal paste on both sides of the device, contact pressure, and ambient conditions) in the measurements.

#### 4.4. TEC module measurement

In order to validate the system further, a commercial TEC of  $8.99 \times 8.99 \text{ mm}^2$  from Adaptive (ET-017-08-15) is used and its cooling performance is measured using the developed system. The measurement is recorded in the ambient environment with a fixed contact pressure of 50 kPa and  $25 \text{ }^\circ\text{C}$  of the hot side temperature. Fig. 9 (a & b) shows the experimental and manufacturer's data sheet provided values for Coefficient of Performance ( $COP$ ) and cooling power ( $Q_c$ ). It can be seen that at lower currents (0.5 & 0.75 A), the measured values are in superposition with the reported values for both  $COP$  as well as  $Q_c$ . In both cases, noticeable deviations are observed at higher currents. At 0.5 A,  $COP$ , cooling power (maximum heat load) ( $Q_c$ ), cold side temperature, hot side temperature, room temperature, and temperature difference

between the hot side and cold side are recorded for about 11 min and the responses are shown in Fig. 9(c). In order to measure the maximum cooling power  $Q_{max}$  ( $Q_c = Q_{max}$  at  $\Delta T = 0 \text{ K}$  across the TEC), a heat load ( $Q_c$ ) of 0.965 W is applied from the hot bar when the input current to the TEC is 0.5 A and the hot side of the TEC is fixed at  $25 \text{ }^\circ\text{C}$ . However, because of the practical uncertainty, the measured result shows minimum deviation from absolute zero condition and the actual  $\Delta T$  is within  $\pm 0.06 \text{ K}$  as shown in Fig. 9(c). The performance of the TEC is also affected by the noise factors, which are ambient temperature, atmospheric pressure, and wind speed. During our measurements, the room temperature is fluctuating between  $24.0$  and  $24.5 \text{ }^\circ\text{C}$ . This implies that the environmental factors have a significant effect on the TEC performance at higher input current.

For a TEC, the cooling performance ( $COP$  and  $Q_c$ ) measurements vary by  $\Delta T$  across the TEC and hot side temperature ( $T_h$ ). As in our system, we are using a commercial  $\mu$ -TEC as a cooling source to maintain the hot side temperature of the measured TEC, we can fix this hot side temperature ( $T_h$ ) over a range of values. Moreover, measurement can be done at different  $\Delta T$  across the TEC.

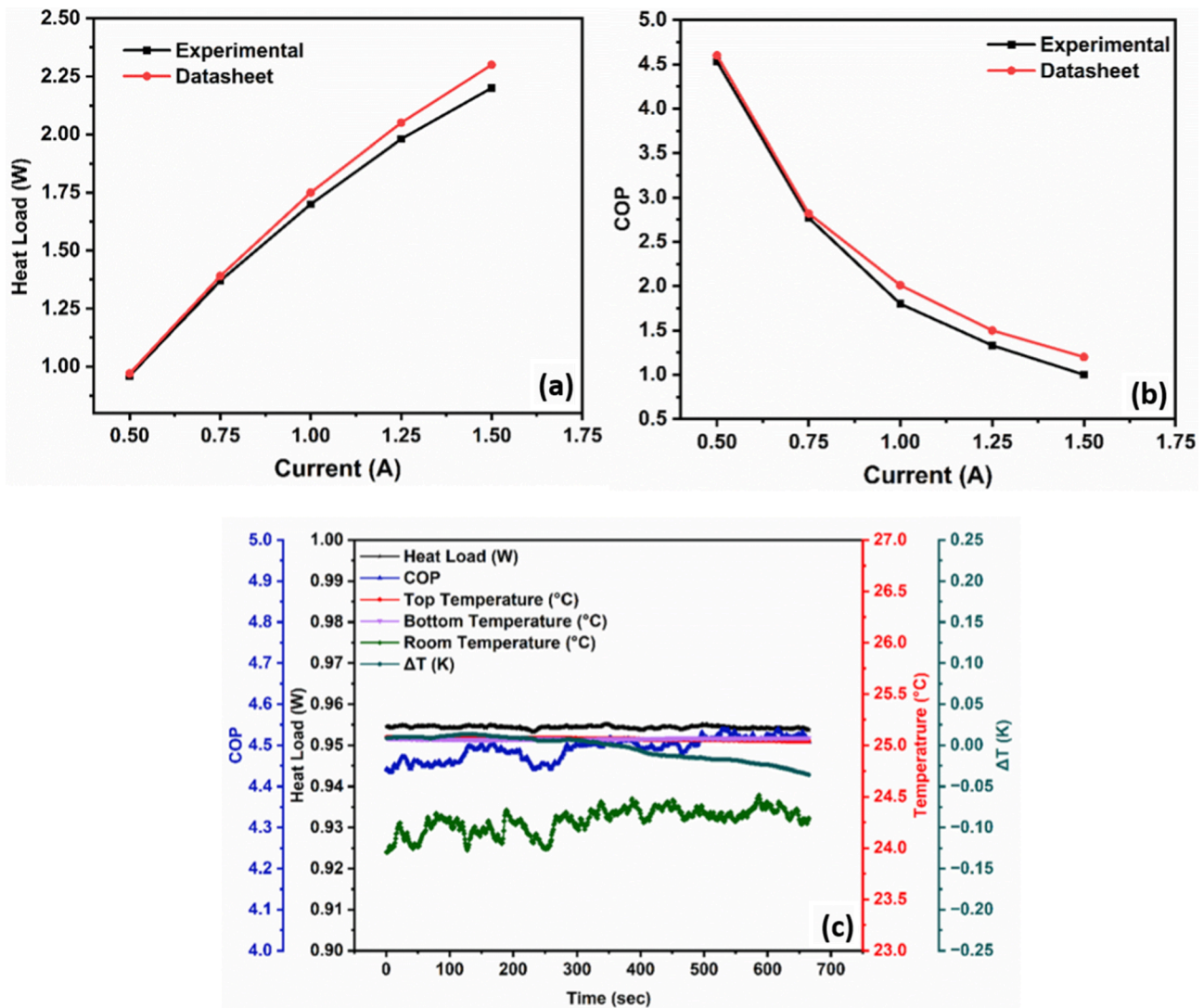


Fig. 9. (a) Cooling power ( $Q_c$ ) and (b)  $COP$  of TEC for five different input currents. (c)  $COP$ , maximum heat load ( $Q_c$ ), cold side temperature, hot side temperature, room temperature and temperature difference between the hot side and cold side are recorded for an applied current of 0.5 A.

## 5. System features and limitations

The advanced thermoelectric devices require accurate performance testing to appraise improvements as compared to existing devices. The developed characterization system follows the ASTM D5470-06 standard and can be able to assess the performance of the macro to micro scale thermoelectric devices non-destructively. The system is capable of characterizing both micro thermoelectric generators and coolers. More specifically, parametric measurements including effective Seebeck coefficient, internal electrical resistance, thermal resistance/conductivity, power output, output voltage, coefficient of performance and cooling power can be evaluated within the minimum deviation limit. Furthermore, the measurements are robust, fast, reliable and precisely controllable. The system operation is enabled via a simple data acquisition system (DAQ card) by dedicated LabVIEW software platform, which allows the user to operate the system automatically over a wide temperature and pressure range, while all measurements are recorded in real time. The measured values using this experimental setup showed good agreement with the manufacturer data and the measurement uncertainty is comparatively low (<4%). In this setup, the measurable size of the TEDs is limited to  $8.79 \times 8.79 \text{ mm}^2$ , which can be further increased by varying the diameter of the meter bars. The operating temperature for the current system is limited to a maximum temperature

gradient of <100 K due to the macro-thermoelectric cooler, which is used as a cooling source. However, this temperature range can be extended to higher temperatures by replacing the cooling source with a high-power cooler coupled with a benchtop temperature controller. Finally, the absence of radiation shield and vacuum/inert environment generate uncertainties in the measurements at high temperature, which can be further reduced by a compact packing of the system under vacuum or inert gas environments to extend the system to commercial standard. In this direction, further improvements and development in the system are in progress and will ensure its suitability for accurate evaluation of thermoelectric device performance.

## 6. Conclusion

In summary, a low-cost robust micro-thermoelectric device ( $\mu$ -TED) measurement system has been developed based on the ASTM D5470-06 standard with user-friendly control interface using LabVIEW software. The system has good capability to measure the output performance like open circuit voltage, short circuit current, internal electrical resistance as a function of temperature, thermal resistivity/conductivity of the device, effective Seebeck coefficient, power output, energy conversion efficiency of a TEG module and coefficient of performance and cooling power of a TEC device. The fully automatic LabVIEW programme have



some special features like automatic temperature stability and maintain the pressure and temperature gradient across the device by accepting user's single input. Moreover, it also allows users to monitor and record the output parameters of the TED module more reliably and accurately. The sensitivity and precision of the system is determined, and the system can maintain a temperature gradient with the accuracy less than  $\pm 0.1$  K. The system has been validated by measuring the thermal conductivity of standard Al disks and observed a deviation of only 0.53% from the reported value in the datasheet. The system is further validated by measuring the temperature dependent performance of a commercially available TEG device of size  $8.79 \times 8.79 \text{ mm}^2$ . It is confirmed that the developed system has good accuracy and acceptable repeatability with less than 4% error. Moreover, TEC performance is also validated using a commercial TEC device. Both COP and cooling power shows good agreement with the datasheet at low applied currents. However, a little deviation can be seen in the measured values due to the environmental factors such as ambient temperature and pressure. However, this deviation can be further reduced by putting the whole system into vacuum chamber. Thereby, this fully automated micro-TED characterization system can be of great assistance in the development and full characterization of the future thermoelectric devices.

### Declaration of Competing Interest

The authors declare that they have no known competing financial interests or personal relationships that could have appeared to influence the work reported in this paper.

### Data availability

Data will be made available on request.

### Acknowledgement

This work received funding from the European Union's Horizon 2020 Research and Innovation Programme under Grant Agreement No. 825114 (SmartVista) and 964251 (TRANSLATE). This publication emanated from research supported in part by a research grant from Science Foundation Ireland (SFI) and was co-funded under the European Regional Development Fund under Grant Number 15/IA/3160, 12/RC/2276 and 13/RC/2077.

### References

- [1] J. Yan, X. Liao, D. Yan, Y. Chen, Review of micro thermoelectric generator, *J. Microelectromech. Syst.* 27 (1) (2018) 1–18.
- [2] Y. Yu, Z. Guo, W. Zhu, J. Zhou, S. Guo, Y. Wang, Y. Deng, High-integration and high-performance micro thermoelectric generator by femtosecond laser direct writing for self-powered IoT devices, *Nano Energy* 93 (2022), 106818.
- [3] Y.J. Kim, H.M. Gu, C.S. Kim, H. Choi, G. Lee, S. Kim, K.K. Yi, S.G. Lee, B.J. Cho, High-performance self-powered wireless sensor node driven by a flexible thermoelectric generator, *Energy* 162 (2018) 526–533.
- [4] J. Kim, S. Khan, P. Wu, S. Park, H. Park, C. Yu, W. Kim, Self-charging wearables for continuous health monitoring, *Nano Energy* 79 (2021), 105419.
- [5] A. Tanwar, S. Lal, K.M. Razeeb, Structural design optimization of micro-thermoelectric generator for wearable biomedical devices, *Energies* 14 (8) (2021) 2339.
- [6] N. Van Toan, T.T.K. Tuoi, T. Ono, Thermoelectric generators for heat harvesting: from material synthesis to device fabrication, *Energ. Convers. Manage.* 225 (2020), 113442.
- [7] N. Van Toan, T. Thi Kim Tuoi, N. Van Hieu, T. Ono, Thermoelectric generator with a high integration density for portable and wearable self-powered electronic devices, *Energy Conversion and Management* 245 (2021) 114571.
- [8] M.N. Hasan, M. Nafea, N. Nayan, M.S. Mohamed Ali, Thermoelectric Generator: Materials and Applications in Wearable Health Monitoring Sensors and Internet of Things Devices, *Advanced Materials Technologies n/a(n/a)* 2101203.
- [9] T. Dasgupta, A.M. Umarji, Apparatus to measure high-temperature thermal conductivity and thermoelectric power of small specimens, *Rev. Sci. Instrum.* 76 (9) (2005), 094901.
- [10] D. Kraemer, G. Chen, A simple differential steady-state method to measure the thermal conductivity of solid bulk materials with high accuracy, *Rev Sci Instrum* 85 (2) (2014), 025108.
- [11] D. Liu, Q. Li, W. Peng, L. Zhu, H. Gao, Q. Meng, A.J. Jin, Developing instrumentation to characterize thermoelectric generator modules, *Rev. Sci. Instrum.* 86 (3) (2015), 034703.
- [12] J. Hejtmánek, K. Knížek, V. Švejda, P. Horna, M. Sikora, Test system for thermoelectric modules and materials, *J. Electron. Mater.* 43 (10) (2014) 3726–3732.
- [13] D. Beretta, M. Massetti, G. Lanzani, M. Caironi, Thermoelectric characterization of flexible micro-thermoelectric generators, *Rev. Sci. Instrum.* 88 (1) (2017), 015103.
- [14] A. Nozariasbmarz, R.A. Kishore, W. Li, Y. Zhang, L. Zheng, M. Sanghadasa, B. Poudel, S. Priya, Thermoelectric coolers for high-power-density 3D electronics heat management, *Appl. Phys. Lett.* 120 (16) (2022), 164101.
- [15] A. Tanwar, R. Kaur, S. Lal, K.M. Razeeb, Finite Element Analysis of Miniature Thermoelectric Cooler for the Thermal Management of Si-Based Photonic Integrated Circuits, *ECS Meeting Abstracts MA2021-02(45)* (2021) 1395-1395.
- [16] S. Lal, D. Gautam, K.M. Razeeb, Fabrication of micro-thermoelectric cooler for the thermal management of photonic devices, *2018 IEEE 18th International Conference on Nanotechnology (IEEE-NANO)*, 2018, pp. 1-2.
- [17] S. Corbett, D. Gautam, S. Lal, K. Yu, N. Balla, G. Cunningham, K.M. Razeeb, R. Enright, D. McCloskey, Electrodeposited thin-film micro-thermoelectric coolers with extreme heat flux handling and microsecond time response, *ACS Appl. Mater. Interfaces* 13 (1) (2021) 1773–1782.
- [18] G. Bulman, P. Barletta, J. Lewis, N. Baldasaro, M. Manno, A. Bar-Cohen, B. Yang, Superlattice-based thin-film thermoelectric modules with high cooling fluxes, *Nat. Commun.* 7 (1) (2016) 1–7.
- [19] G.J. Snyder, J.R. Lim, C.-K. Huang, J.-P. Fleurial, Thermoelectric microdevice fabricated by a MEMS-like electrochemical process, *Nat. Mater.* 2 (8) (2003) 528–531.
- [20] G. Li, J. Garcia Fernandez, D.A. Lara Ramos, V. Barati, N. Pérez, I. Soldatov, H. Reith, G. Schierning, K. Nielsch, Integrated microthermoelectric coolers with rapid response time and high device reliability, *Nat. Electron.* 1 (10) (2018) 555–561.
- [21] ASTM, Standard test method for thermal transmission properties of thermally conductive electrical insulation materials, (2012).
- [22] J. Xu, A. Munari, E. Dalton, A. Mathewson, K.M. Razeeb, Silver nanowire array-polymer composite as thermal interface material, *J. Appl. Phys.* 106 (12) (2009), 124310.
- [23] R. Kempers, P. Kolodner, A. Lyons, A.J. Robinson, A high-precision apparatus for the characterization of thermal interface materials, *Rev. Sci. Instrum.* 80 (9) (2009), 095111.